

Water Vapor Sorption and Transport in Dense Polyimide Membranes

Jingui Huang,¹ Richard J. Cranford,² Takeshi Matsuura,³ Christian Roy^{1,2}

¹Department of Chemical Engineering, Laval University, Ste-Foy, Québec, Canada G1K 7P4

²Institut Pyrovac, Incorporated, Parc Technologique du Québec Métropolitain, 333 Rue Franquet, Ste-Foy, Québec, Canada G1P 4C7

³Industrial Membrane Research Institute, Department of Chemical Engineering, University of Ottawa, Ontario, Canada K1N 6N5

Received 27 September 2001; accepted 24 May 2002

ABSTRACT: The sorption and transport of water vapor in five dense polyimide membranes were studied by thermogravimetry. The sorption isotherms of water vapor in the polyimides could be successfully interpreted by both the dual-mode sorption model and the Guggenheim–Anderson–de Boer equation. The water vapor diffusion behavior was found to be nearly Fickian at higher water vapor activities, whereas non-Fickian diffusion was observed at lower water activities. The phenomena could be well described by the mechanism of combined Fickian and time-dependent diffusion. The diffusion coefficient and water vapor uptake in the polyimides were strongly dependent on the polymer molecular structure. Except for the polyimide prepared from 3,3',4,4'-diphenylsulfone

tetracarboxylic dianhydride and 1,3-bis(4-aminophenoxy) benzene, the permeability of water vapor in the dense polyimide membranes predicted from the sorption measurement at 30°C corresponded well with the water vapor permeability measured at 85°C. Among the polyimides studied, pyromellitic dianhydride–4,4'-diaminophenylsulfone (50 mol%)/4,4'-oxydianiline (50 mol%) showed both high water sorption and diffusion and, therefore, high water vapor permeability, which for vapor permeation membranes is necessary for the separation of water vapor from gas streams. © 2003 Wiley Periodicals, Inc. *J Appl Polym Sci* 87: 2306–2317, 2003

Key words: polyimides; membranes; diffusion; films

INTRODUCTION

Water vapor separation membranes have attracted great interest because of their applications for the dehumidification of gases, air, and organic vapors.^{1,2} In the development of membranes for the separation of water vapor from organic compounds, especially for the treatment of byproduct streams in wood drying or pyrolysis processes, the thermal and chemical resistance of membranes is of primary importance.^{3,4} Polyimides, with their excellent thermal, mechanical, and chemical properties, have been widely used in the microelectronics and aerospace industries, and they have also attracted much attention as gas separation membranes since the early 1970s because of their high separation factors.^{5–8} Because of their high permeability to water vapor, polyimides are also considered to be applicable as membranes for water vapor separation.^{9–11}

Water sorption in polyimides is an important factor for many practical applications because the extent of water sorption determines the polymer properties and their applications in working environments. For instance, in the electronic, composite, or adhesive applica-

tions of polyimides, the use of a polyimide largely depends on its low permeation to water vapor because sorbed water not only affects performance but also causes metal corrosion, adhesion failure, and degradation of dielectric properties.^{6,12} Therefore, studies of the sorption and permeation of water vapor in several polyimides have been made, including the widely used commercial polyimide films.^{6,13–15} However, in the development of polyimides as vapor separation membranes, particularly for the separation of water vapor from gas streams containing various organic compounds, a polyimide resistant to organic solvents and having high water sorption and transport characteristics, as well as good water separation performance, is desired. However, very little information is currently available for such applications. Therefore, the purpose of this study is to evaluate the sorption and transport behavior of water vapor in solvent-resistant polyimides with different molecular structures because it is a key factor for the design of membrane materials and membranes for the separation of water from gas streams.

BACKGROUND AND THEORY

Sorption isotherms

The sorption isotherms of small molecule penetrants (gases or vapors) in many glassy polymers are con-

Correspondence to: C. Roy (croy@gch.ulaval.ca).

cave to the activity or relative pressure axis and are generally described by the dual-mode sorption model.^{9,16,17} This model postulates that the sorbed penetrant exists in two populations: one is dissolved in the polymer matrix according to Henry's law, and the other is considered to occupy unrelaxed free volume within the polymer according to the Langmuir isotherm. The dual-mode sorption isotherm is given as follows:

$$C = C_D + C_H = k_D p + \frac{C'_H b p}{1 + b p} \quad (1)$$

where C is the solubility of the penetrant in the polymer [$\text{m}^3(\text{STP})/\text{m}^3(\text{polymer})$]; C_D represents the sorption of normally diffusible species; C_H represents the sorption of species in microvoids or holes in the polymer matrix; k_D is the Henry's law dissolution constant [$\text{m}^3(\text{STP})/\text{m}^3(\text{polymer}) \text{Pa}$]; b is the affinity constant of the gas or vapor for the Langmuir sites, or so-called hole affinity constant (Pa^{-1}); C'_H is the maximum capacity of the polymer for the penetrant in the Langmuir sorption sites; and p is the gas or vapor pressure (Pa).

The temperature dependence of k_D and b can be estimated by the van't Hoff analysis:^{17,18}

$$k_D = k_{D0} \exp\left(-\frac{\Delta H_D}{RT}\right) \quad (2)$$

$$b = b_0 \exp\left(-\frac{\Delta H_b}{RT}\right) \quad (3)$$

where ΔH_D is the enthalpy of sorption in Henry's mode, ΔH_b is the enthalpy of sorption in the Langmuir sites, k_{D0} is a pre-exponential factor, b_0 is a pre-exponential factor, T is the absolute temperature, and R is the gas constant.

Concerning water vapor sorption in the dense polyimide membranes studied in this work, the dual-mode sorption model is used to interpret water sorption behaviors in the polyimides. The dual sorption model is known to be one of the most effective models for describing gas and vapor sorption and permeation in glassy polymers, including many polyimides.^{9,10} It, however, exhibits limitations in describing water sorption in some hydrophilic glassy polymers with typical sigmoid isotherms or the so-called type II isotherms, probably because of strong interactions between the penetrant molecules and the polymer materials, which lead to complex isotherms.

An alternative approach to describing water sorption isotherms is the Guggenheim–Anderson–de Boer (GAB) equation:^{19–21}

$$C = \frac{C_m A B a}{(1 - A a)(1 - A a + A B a)} \quad (4)$$

where C is the water content in the polymer at water vapor activity a , C_m is the monolayer moisture content, and A and B are temperature-dependent constants. That is,^{19,20}

$$A = A_0 \exp\left(\frac{H_L - H_n}{RT}\right) \quad (5)$$

$$B = B_0 \exp\left(\frac{H_L - H_m}{RT}\right) \quad (6)$$

where A_0 and B_0 are pre-exponential factors; H_L is the heat of condensation of pure water vapor; and H_m and H_n are the heats of sorption of monolayer and multilayer layers of water, respectively.

Despite having appeared in an article as early as 1946,¹⁹ this GAB equation had rarely been used for modeling water sorption in synthetic or natural polymers for a long time. Quite recently, however, it has been observed that this GAB three-parameter model fit well the water sorption data of food and related natural materials.^{20–22} Therefore, it has been used by some authors to simulate sorption isotherms for polymers with typical type II curvatures.^{23–25} Both the dual-mode sorption model and the GAB equation will be considered for comparison to fit the water sorption data in the polyimide membranes studied.

Sorption kinetics

The kinetic study of the sorption and desorption of gases and vapors in polymers as a means of determining the diffusion coefficient has widely been used. For the study of the transport behavior of relatively non-interacting gases or vapors in glassy polymers, Fick's second law may be applied, with relatively weak interactions assumed between the penetrant molecules and the glassy polymers,^{18,26} even though non-Fickian (case II and anomalous) diffusion is observed in most cases:

$$\frac{\partial C}{\partial t} = \frac{\partial}{\partial x} \left[D \frac{\partial C}{\partial x} \right] \quad (7)$$

where C is the concentration of the penetrant material at time t and at a distance of x from the polymer surface and D is the diffusion coefficient. The solution of eq. (7) is given by the following equation, which has been derived for an infinite slab with a constant diffusion coefficient:²⁶

$$\frac{M_t}{M_\infty} = 1 - \frac{8}{\pi^2} \sum_{m=0}^{\infty} \frac{1}{(2m+1)^2} \exp\left[-\frac{D(2m+1)^2\pi^2 t}{L^2}\right] \quad (8)$$

where M_t is the amount of gas or vapor sorbed at time t , M_∞ is the equilibrium sorption, m is an integer, and L is the film thickness. For short times, the initial mass gain is shown to be proportional to the square root of the time ($t^{1/2}$), and eq. (8) may be approximated as follows:

$$\frac{M_t}{M_\infty} = \frac{4}{L} \left[\frac{D_I t}{\pi} \right]^{1/2} \quad (9)$$

where D_I is the initial diffusion coefficient. For long times, particularly when M_t/M_∞ is greater than 0.5, the rate of mass gain begins to fall noticeably toward the mass gain at equilibrium, and the approximation of eq. (8) is given as follows:

$$\frac{M_t}{M_\infty} = 1 - \frac{8}{\pi^2} \exp\left[-\frac{\pi^2 D_E t}{L^2}\right] \quad (10)$$

where D_E is the diffusion coefficient at equilibrium. Therefore, there are two methods for the calculation of the diffusion coefficient from a sorption kinetic curve. A plot of M_t/M_∞ versus $t^{1/2}$ is initially linear, and from the slope, D_I can be evaluated. Similarly, D_E may be calculated from the slope of $\ln(1 - M_t/M_\infty)$ versus t , with the long-time asymptotic solution of eq. (10) when M_t/M_∞ is greater than 0.5.

The two diffusion coefficients determined theoretically should be the same if the diffusion of a penetrant in the polymer is Fickian. However, in many real systems, deviations from Fick's law occur, particularly in the sorption of organic vapors by most polymers and of water by hydrophilic polymers.²⁷⁻²⁹ The diffusion coefficient is not constant, and in most cases, the deviations from Fick's law cannot be explained by a concentration-dependent diffusion coefficient. The diffusion coefficient is time-dependent, and this is ascribed to the relaxation of the polymer molecular chains. There are several explanations for this non-Fickian diffusion behavior:³⁰

1. In case I diffusion (Fickian), the rate of penetrant diffusion is much less than the rate of relaxation of the polymer material, and the amount of diffused penetrant is proportional to the square root of time, simply expressed by $M = kt^{1/2}$, where k is a constant.
2. In case II diffusion, the rate of penetrant diffusion is much greater than the rate of relaxation of the polymer chain. A sharp penetrant front, which separates the swollen gel region from the glassy

core, advances into the polymer matrix at a constant velocity, ahead of which the concentration of the penetrant drops rapidly, and the amount of weight gain increases linearly with time ($M = kt$).

3. In anomalous diffusion, the rate of diffusion is comparable to the rate of relaxation of the polymer, and the amount of diffused penetrant is related to time up to the power between 0.5 and 1.0, expressed by $M = kt^n$, where $n = 0.5-1.0$.

To examine non-Fickian diffusion, many attempts have been made. Wang et al.³¹ and Kwei et al.³² derived the following equation combining Fickian and case II diffusion:

$$\frac{\partial C}{\partial t} = \frac{\partial}{\partial x} \left[D \frac{\partial C}{\partial x} - vC \right] \quad (11)$$

where the first term in the square brackets describes the simple Fickian diffusion, the second term describes the contribution of the internal stress arising from the polymer, and v is the velocity of case II diffusion.

For the numerical solution of combined diffusion, Berens and Hopfenberg²⁷ introduced a simple diffusion-relaxation model, which allows us to separate diffusion and relaxation effects as follows:

$$M_t = M_{t,D} + M_{t,R} \quad (12)$$

where $M_{t,D}$ is the amount of penetrant sorbed by a Fickian diffusion mechanism, corresponding to eq. (8), and $M_{t,R}$ is the amount of diffusant sorbed by case II diffusion because of relaxation. Furthermore,

$$\frac{M_{t,R}}{M_{\infty,R}} = 1 - \exp(-kt) \quad (13)$$

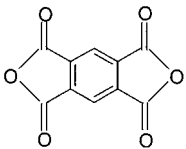
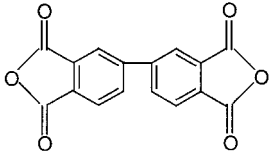
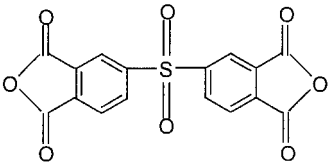
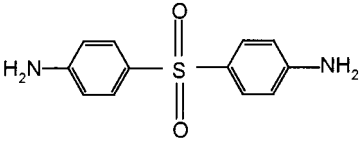
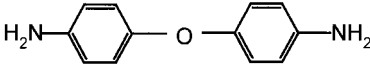
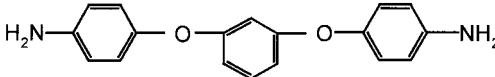
where k is a first-order relaxation rate constant, which is independent of the sample thickness.

Similarly, Toi and coworkers^{33,34} also proposed a model to describe non-Fickian transport behavior by combining Fickian diffusion with Crank and Park's time-dependent model, in which it is assumed that the diffusion coefficient of the penetrant in the glassy polymer at time t (D_t) is related to the short-time and long-time diffusion coefficients determined from eqs. (9) and (10) by the following equation:

$$D_t = D_E - (D_E - D_I)\exp(-\alpha t) \quad (14)$$

where D_I and D_E are diffusion constants for the short term and long term, respectively, and α is the first-order rate constant for the relaxation process. Substituting eq. (14) into eq. (8), we found that many non-

TABLE I
Monomers Used in the Preparation of Polyimides

Monomer	Molecular structure	Melting point (°C)
PMDA		285
BPDA		300
DSDA		287
DDS		176
ODA		192
TPER		116

Fickian sorption behaviors of various gases in glassy polyimides could be successfully interpreted by a model in which time-dependent diffusion and the Fickian model were combined.

In this work, the Fickian diffusion model and the time-dependent short-time and long-time diffusion coefficient model are used to analyze the experimental results.

Water vapor permeability

The permeation of gas or vapor penetrants through polymer membranes is characterized by a permeability coefficient (P):^{2,35}

$$P = \frac{J}{(p_2 - p_1)/L} \quad (15)$$

where p_2 and p_1 are the upstream and downstream pressures of the gas or vapor permeating a membrane of thickness L . J is the steady-state flux of the gas or vapor for one-dimensional Fickian diffusion.

The permeation of gases or vapors through a dense or nonporous membrane is a solution-diffusion process. Therefore, P can be separated as a product of an

average diffusion coefficient (\bar{D}) and a solubility coefficient (S) via

$$P = \bar{D}S \quad (16)$$

which may be evaluated from the sorption isotherm and the permeation experimental measurements.

EXPERIMENTAL

Materials and sample preparation

The molecular structures of the monomer dianhydrides and diamines used in this study are given in Table I. All the monomers used were obtained from Chriskev Co. (Leawood, KS). The dianhydrides [pyromellitic dianhydride (PMDA), 3,3',4,4'-biphenyl tetracarboxylic dianhydride (BPDA), and 3,3',4,4'-diphenylsulfone tetracarboxylic dianhydride (DSDA)] were recrystallized from acetic anhydride, dried at 220–250°C in N_2 for 3–5 h, and stored in a desiccator over silica gel before use. The diamines [4,4'-oxydianiline (ODA), 4,4'-diaminodiphenylsulfone (DDS), and 1,3-bis(4-aminophenoxy)benzene (TPER)] were recrystallized from ethanol and vacuum-dried. *N*-Methyl-2-

pyrrolidone (NMP) was dehydrated successively with CaSO_4 and phosphorus pentoxide and then was vacuum-distilled before use.

Poly(amic acid) precursors were prepared by the solution condensation of an aromatic dianhydride with a stoichiometric amount of one or two aromatic diamines in NMP. Dense polyimide films were prepared by the spin coating of 8–12 wt % poly(amic acid) precursors onto glass plates. The films were dried at 70°C for 1.5 h and subsequently cured under flowing nitrogen at 100°C for 1 h, at 200°C for 2 h, and at 300°C for 1 h. After cooling to room temperature, the fully cured dense polyimide films were taken off from the glass substrates with the aid of water and were then washed several times with distilled water and later dried at 140°C under flowing N_2 for 24 h. The thickness of the films was determined by the weighing of a film of known area and was verified by scanning electron microscopy. The density of the polyimide films prepared was measured in kerosene and compared with the flotation method with calcium nitrate/water solutions: PMDA-50DDS/50ODA (DDS, 50 mol%; ODA, 50 mol%), 1.415 g/cm³; BPDA-50DDS/50ODA, 1.384 g/cm³; BPDA-DDS, 1.411 g/cm³; BPDA-ODA, 1.370 g/cm³; and DSDA-TPER, 1.394 g/cm³. The films were cut into rectangular pieces (ca. 8 mm × 12 mm) and fully dried in a vacuum oven before being used for gravimetric measurements. For water vapor permeation tests, circular films with a diameter of around 80 mm were used. The effective area of the film for permeation was 28.26 cm².

Measurements

The stability of the polyimides in an organic environment was characterized by membrane samples being immersed in a strong solvent such as NMP and kept in the solvent for several days so that it could be observed if the samples were dissolved or partially dissolved or swollen. Among the membranes prepared, PMDA- and BPDA-based membranes showed good solvent resistance, whereas DSDA-based membranes were dissolved or partially dissolved in the solvent NMP.

The water sorption in the dense polyimide membranes was measured by a gravimetric method. The microbalance in the thermogravimetric analyzer (TG/TGA 220, Seiko Instruments, Japan; Supplied by Thermo Haake, NJ) was used; this is similar to the method that Shigetomi et al.³⁶ described in the literature. Membrane samples were vacuum-dried at 140°C for 24 h before the tests. The film specimens were set to stand on an aluminum sample pan, in which two V-shape gaps were cut from the top to the bottom along the diameter of the pan to hold the samples stable. N_2 was used as a carrier gas that was forced to

bubble through a thermostated saturation vessel and fed into the sample chamber. Heating tape and insulation were wrapped around the tubing inlet system so that vapor condensation in the apparatus could be avoided. The water vapor uptake at a given vapor activity (which was assumed equal to the relative vapor pressure, p/p_s , where p_s is the water vapor saturation pressure at a given temperature) was automatically recorded. For each sample, measurements were made several times, and before each measurement, the sample was dried at 140°C with dry nitrogen flowing for at least 10 h.

The permeation tests of water vapor in the dense polyimide membranes were carried out with a laboratory test cell,^{3,8} in which the water vapor was generated by the pumping of pure water through a preheating tubing that was heated to 140–160°C for the evaporation of water. Water vapor was introduced to the membrane test unit at a given temperature and feed pressure through long, circular tubing placed in a constant-temperature oven. Dense polyimide membranes were tested at 85°C. Feed and permeate pressures were controlled at 40 and 1.5–2 kPa, respectively. The retentate vapor was condensed by a condenser cooled by ice-cold water, and the permeate vapor was condensed by a trap cooled by acetone/dry ice. After the membranes were equilibrated for 6–8 h in water vapor, the permeate samples were collected, under the assumption that steady-state conditions were reached.

RESULTS AND DISCUSSION

Sorption isotherms

The sorption isotherms of dense polyimide membranes determined from the mass gains at different water vapor activities at 30°C are shown in Figure 1. All the isotherms are concave to the activity axis at low water activity and are almost linear at high activity. These sorption behaviors can be satisfactorily described by the dual-mode sorption model via eq. (1). The values of the dual-mode sorption parameters that appear in eq. (1) have been obtained, and the results are listed in Table II. The solid lines shown in Figure 1(a) are theoretical lines based on the parameters given in Table II, and they are in good agreement with the experimental data.

It can be seen from Table II that PMDA-50DDS/50ODA shows both large values of k_D and b and a small value of C_H' in comparison with other polyimides. The large values of both k_D and b and the small value of C_H' cause the sorption isotherm to deviate appreciably from the Henry's law isotherm only in the lower water vapor activity region. The large values of both k_D and b in polyimide PMDA-50DDS/50ODA

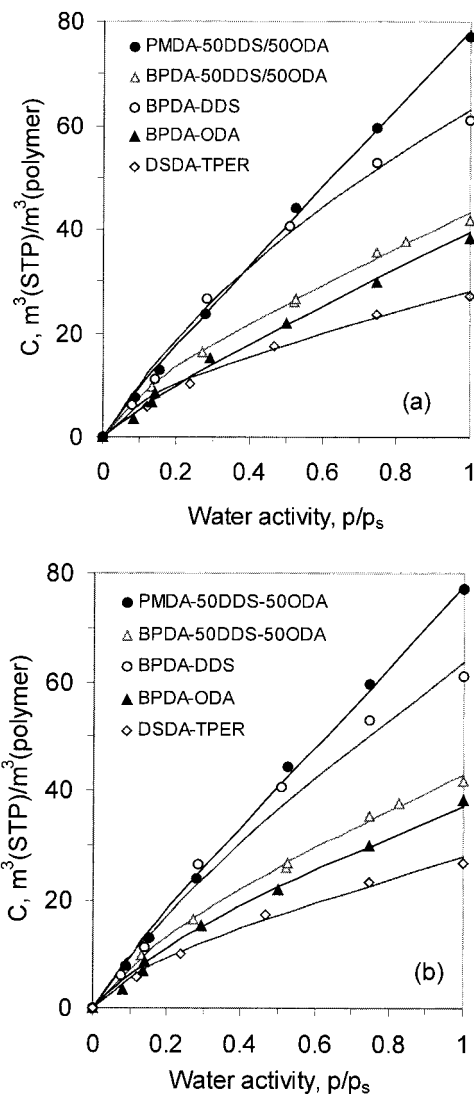


Figure 1 Sorption isotherms of water vapor in dense polyimide membranes at 30°C. Symbols represent observed values, and lines represent calculated values from (a) the dual-mode model and (b) the GAB model.

are suggestive of strong interactions between polymer molecular chains and water molecules that may be attributed to the introduction of polar sulfonyl ($-\text{SO}_2-$) connection groups into the molecular chains. However, with respect to BPDA-DDS and DSDA-TPER, the affinity constant for the former is relatively low, and k_D is not high for DSDA-TPER in

TABLE III
GAB Model Parameters for Water Vapor in Dense Polyimide Membranes at 30°C

Polyimide	C_m [m^3 (STP)/ m^3 (polymer)]	A	B
PMDA-50DDS/50ODA	75	0.35	3.9
BPDA-50DDS/50ODA	40	0.30	7.0
BPDA-DDS	66	0.29	5.3
BPDA-ODA	35	0.30	6.7
DSDA-TPER	22	0.35	8.5

comparison with the values of other polyimides in this study, even though they all contain the sulfonyl connector groups (i.e., for BPDA-DDS in the diamine unit and for DSDA-TPER in the dianhydride moiety). It has been said that the sulfonyl connector groups in the dianhydride may have greater influence on the solubility of membranes prepared,³⁷ as evidenced in this study by the DSDA-TPER dense membrane, which shows poor solvent resistance to the organic solvent NMP. Correspondingly, the affinity constant of DSDA-TPER is as high as $1.6 \times 10^{-3} \text{ Pa}^{-1}$ (Table II), but M_∞ for water vapor is the lowest among the polyimides studied because of the low k_D value.

Figure 1(b) shows water vapor sorption isotherms of the polyimide membranes fit by the GAB equation via eq. (4). The three parameters in the GAB equation have been estimated by the best fitting of the model to the experimental data and are given in Table III. The symbols shown in Figure 1(b) are experimental data observed, whereas the solid lines are calculated from the GAB equation based on the parameters shown in Table III. The fitting is very good except for BPDA-DDS.

The parameters C_m , A , and B in the GAB equation depend on the polymer characteristics and the temperature. At a given temperature, these parameters are mainly determined by the polymer characteristics. From Table III, it can be seen that all the values of A are small, less than 0.4, and this indicates that water vapor sorption in the polyimides is almost entirely confined to the first and second layers.¹⁹ However, the value of C_m changes significantly. PMDA-50DDS/50ODA exhibits the highest value of C_m , whereas DSDA-TPER shows the lowest; this suggests that PMDA-50DDS/50ODA has the largest water vapor

TABLE II
Dual-Mode Sorption Parameters for Water Vapor in Dense Polyimide Membranes at 30°C

Polyimide	$k_D \times 10^3$ [m^3 (STP)/ m^3 (polymer) Pa]	C_H [m^3 (STP)/ m^3 (polymer)]	$b \times 10^4$ (1/Pa)
PMDA-50DDS/50ODA	17.26	4.93	30
BPDA-50DDS/50ODA	7.76	12.06	15
BPDA-DDS	7.03	54.48	3.7
BPDA-ODA	8.02	6.99	9
DSDA-TPER	4.34	11.11	16

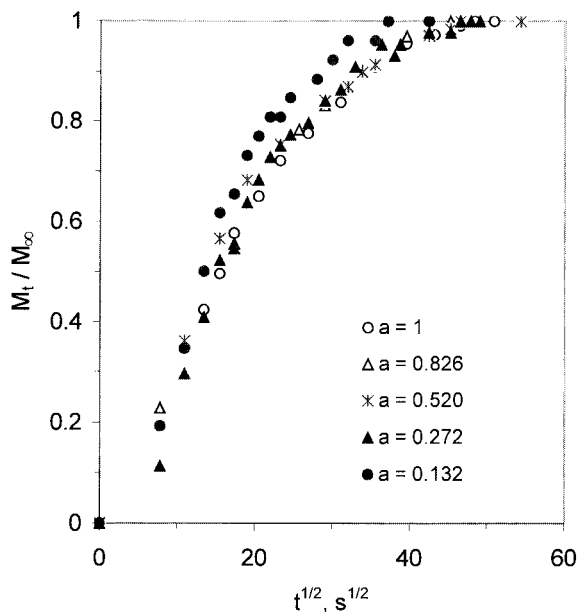


Figure 2 Sorption kinetics of water vapor in dense polyimide BPDA-50DDS/50ODA membranes at 30°C.

sorption capacity among the polyimide membranes studied. This is quite reasonable if we consider the much higher water sorption of PMDA-50DDS/50ODA with respect to the other polyimides investigated. The larger value of C_m in PMDA-50DDS/50ODA is probably due to the introduction of polar sulfonyl ($-\text{SO}_2-$) connection groups into the molecular chains, which are, however, more rigid than other polyimide molecular chains because of the rigid and short dianhydride PMDA moiety. Therefore, PMDA-50DDS/50ODA has a more open structure, and this results in the exposure of more binding sites for water vapor sorption. The constant B in the GAB equation is related to the interaction energy of water vapor and the polymeric material. For a strongly adsorbent substance, $B \gg 1$. In Table III, it can be seen that PMDA-50DDS/50ODA displays the highest value of C_m and the lowest value of B , and this implies that PMDA-50DDS/50ODA contains more sorbing sites but much weaker binding strength between the water and polymer in comparison with other polyimides. These characteristics are preferable for water vapor permeation membranes because the sorbed water in the membrane would be much easier to separate from the membrane. For DSDA-TPER, the lowest value of C_m and the highest value of B are observed, and this suggests a smaller number of active sorbing sites for water vapor but much stronger binding strength between the water and polymer. These seem to be the least undesirable characteristics of a membrane material to be used for water vapor permeation.

In short, the water vapor sorption behaviors in the polyimide membranes investigated could be satisfac-

torily described by both the dual-mode sorption model and the GAB equation.

Sorption kinetics

The sorption kinetics of water vapor in dense polyimide membranes were gravimetrically measured at different water vapor activities. M_t/M_∞ values are plotted versus $t^{1/2}$ in Figure 2 for a dense polyimide BPDA-50DDS/50ODA membrane at water vapor activities of 0.132–1.0 at 30°C. The purely Fickian diffusion model seems to provide an excellent description for the sorption of water vapor in the membrane at higher water vapor activities, as shown in Figure 3. These sorption behaviors are also found in other polyimides, as shown in Figure 4. The solid lines in Figures 3 and 4 have been calculated from eq. (8) with a constant diffusion coefficient for each sample at the given test conditions: $4.5 \times 10^{-14} \text{ m}^2/\text{s}$ for BPDA-50DDS/50ODA in Figures 3 and 4 and $1.6 \times 10^{-13} \text{ m}^2/\text{s}$ for PMDA-50DDS/50ODA, $3.8 \times 10^{-14} \text{ m}^2/\text{s}$ for BPDA-DDS, $2.0 \times 10^{-14} \text{ m}^2/\text{s}$ for BPDA-ODA, and $1.6 \times 10^{-13} \text{ m}^2/\text{s}$ for DSDA-TPER in Figure 4. However, deviations from the ideal model appear when the membranes are investigated at lower water vapor activities. These sorption behaviors are somewhat different from other observations for the sorption of permanent gases and organic solvents in glassy films,¹⁷ for which deviations from Fickian diffusion occurred at higher activities of gas or vapor penetrants and were ascribed to the superimposition of some relaxation processes on the diffusion process.

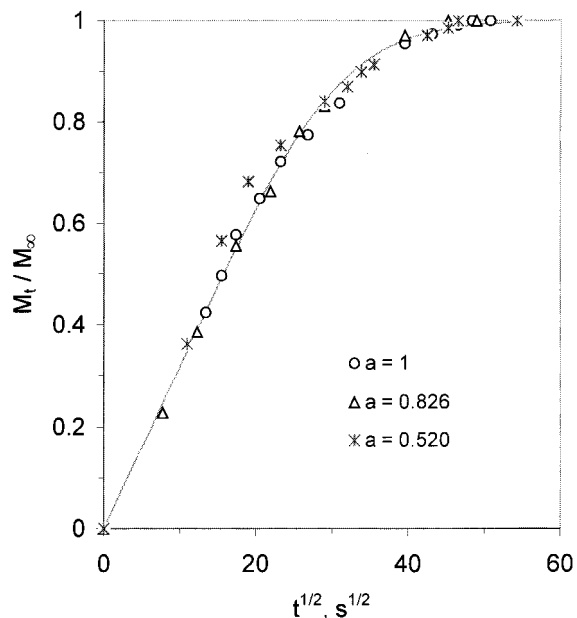


Figure 3 Sorption kinetics of water vapor in dense polyimide BPDA-50DDS/50ODA membranes at higher water vapor activities and at 30°C. Symbols represent observed values, and lines represent calculated values from eq. (8).

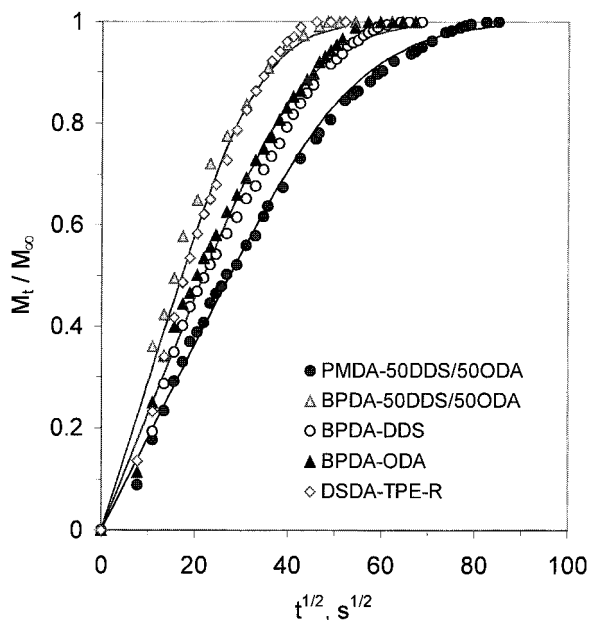


Figure 4 Sorption kinetics of water vapor in dense polyimide membranes at 30°C ($p/p_s = 1$). Lines represent calculated values from eq. (8).

Generally, the non-Fickian sorption and transport of water vapor in the glassy polymers are considered to be somewhat related to the interaction of polar water with the polymer or water molecule itself because water molecules may interact with the polymer to act as plasticizers or with each other to form clusters. However, a Zimm–Lundberg analysis^{38,39} of the sorption isotherms (Fig. 1) indicated the absence of clustering, as the clustering function is far less than -1 for all the polyimides in the range of water vapor activities studied. Therefore, the deviations from the Fickian diffusion of water vapor in the polyimides may be related to the plasticization of water to the membrane. It was suggested that some relaxation process was superimposed on the diffusion process because of the plasticization of water vapor in the polyimide even at low water activities. Berens and Hopfenberg²⁷ proposed a phenomenological model that permits the separation of diffusion and relaxation effects. Toi and coworkers^{33,34} used the two diffusion coefficients determined from eqs. (9) and (10) in combination with Crank and Park's time-dependent model to describe the non-Fickian transport behaviors of several gases in polyimide films. A similar approach was applied in this study for the sorption and transport of water vapor in the glassy dense polyimide membranes.

In Figure 5, data for the two lowest water vapor activities are shown together with theoretical lines that were calculated by eq. (8) and based on the time-dependent diffusion coefficients obtained from eq. (14) with a best fit value for α . D_I and D_E , required in eq. (14), were obtained from eqs. (9) and (10), respec-

tively. The fitting seems to be excellent. All the diffusion coefficients obtained by the aforementioned curve-fitting method, along with α , are summarized in Table IV. In Table IV, it can be seen that the sorption kinetics of water vapor in polyimides are quite different from one to another and seem to be strongly dependent on the structure of the polyimide. The wide scatter found in D_I and D_E makes the comparison of the polyimides difficult in the low water vapor activity range. However, at higher water vapor activities, for example, at $p/p_s = 1$, the D value for water vapor varies from $2.0 \times 10^{-14} \text{ m}^2/\text{s}$ to $1.6 \times 10^{-13} \text{ m}^2/\text{s}$, and it occurs in the following order: BPDA-ODA < BPDA-DDS < BPDA-50DDS/50ODA < DSDA-TPER = PMDA-50DDS/50ODA. The water uptake varies from 1.57 to 4.37 wt % and is in the increasing order: DSDA-TPER < BPDA-ODA < BPDA-50DDS/50ODA < BPDA-DDS < PMDA-50DDS/50ODA.

Effect of temperature on the water sorption behavior

The effect of temperature on water vapor sorption in the dense polyimide membranes was investigated at a constant water vapor pressure of 3168 Pa. The results are illustrated in Figure 6. M_∞ for water decreases with an increase in temperature. The data, however, do not follow the van't Hoff relationship in the whole range of temperatures studied, from 30 to 105°C, probably because of the strong interaction of water with the polymer, particularly at lower temperatures (with high water activity).

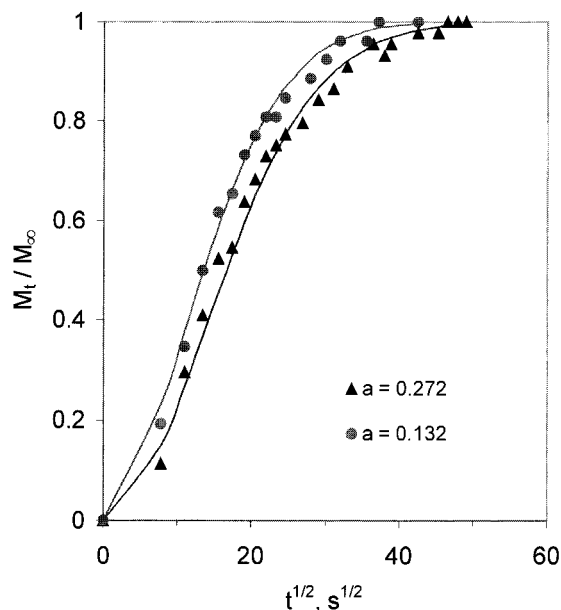


Figure 5 Sorption kinetics of water vapor in dense polyimide BPDA-50DDS/50ODA membranes at lower water vapor activities and at 30°C. Lines represent calculated values from eq. (8), with D determined from eq. (14).

TABLE IV
Diffusion Coefficients and Water Vapor Uptake in Dense Polyimide Membranes at 30°C

Polyimide	Thickness (μm)	Water vapor activity (p/p_s)	Water uptake (wt %)	$D \times 10^{14}$ (Fickian; m^2/s)	$D_1 \times 10^{14}$ (m^2/s)	$D_E \times 10^{14}$ (m^2/s)	α
PMDA-50DDS/50ODA	49.5	0.088	0.43	—	3	120	0.001
		0.154	0.73	—	2.8	1.6	0.001
		0.280	1.35	16			
		0.526	2.51	16			
		0.747	3.39	16			
BPDA-50DDS/50ODA	15.1	1	4.37	16			
		0.132	0.57	—	1.5	7	0.01
		0.272	0.95	—	0.2	5	0.006
		0.520	1.51	5			
		0.526	1.55	5.2			
BPDA-DDS	19.2	0.747	2.06	4.8			
		0.826	2.19	4.5			
		1	2.42	4.5			
		0.078	0.34	—	3.0	15	0.002
		0.140	0.64	9.0			
BPDA-ODA	13.2	0.283	1.51	—	5.0	2.0	0.0012
		0.509	2.30	3.2			
		0.747	3.01	2.9			
		1	3.47	3.8			
		0.082	0.16	7.5			
DSDA-TPER	31.4	0.141	0.49	2.7			
		0.293	0.91	—	2.5	1.3	0.001
		0.501	1.23	—	2.5	1.3	0.001
		0.747	1.75	2.0			
		1	2.25	2.0			
DSDA-TPER	31.4	0.120	0.33	—	1.0	28	0.003
		0.239	0.59	—	1.0	19	0.02
		0.466	1.01	16			
		0.747	1.36	15			
		1	1.57	16			

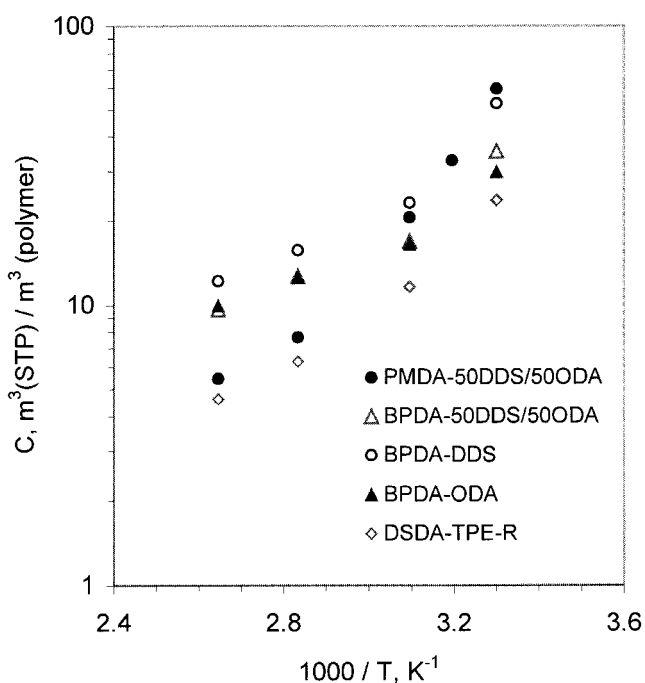


Figure 6 Van't Hoff plots of water vapor sorption in polyimides (water vapor pressure = 3168 Pa).

The diffusion coefficients determined from the sorption kinetics are shown in Figure 7 in the form of an Arrhenius plot. The D_E values obtained from experiments were used for this comparison. For PMDA-50DDS/50ODA, DSDA-TPER, and BPDA-DDS, the diffusion coefficient increases with an increase in temperature in the range of 30–80°C. For BPDA-ODA and BPDA-50DDS/50ODA, the diffusion coefficient is either independent of temperature or increases only slightly with an increase in temperature. At higher temperatures (>80°C), the diffusion coefficient of water vapor in PMDA-50DDA/50ODA does not change with increasing temperature and remains at 4×10^{-13} m^2/s , whereas for BPDA-DDS and BPDA-50DDS/50ODA, there is a decrease in the diffusion coefficient. This is probably because of the effect of antiplasticization of the sorbed water to the polar polyimides, particularly at a relatively low water vapor activity (at a higher temperature), as observed for Kapton polyimide.⁴⁰ The plasticization effect of water vapor on the polyimides is concentration-dependent. Therefore, when the sorbed water is below a certain concentration, water molecules lower the chain mobility and suppress sub-glass-transition-temperature segmental motion, resulting in lower diffusion coefficients. The

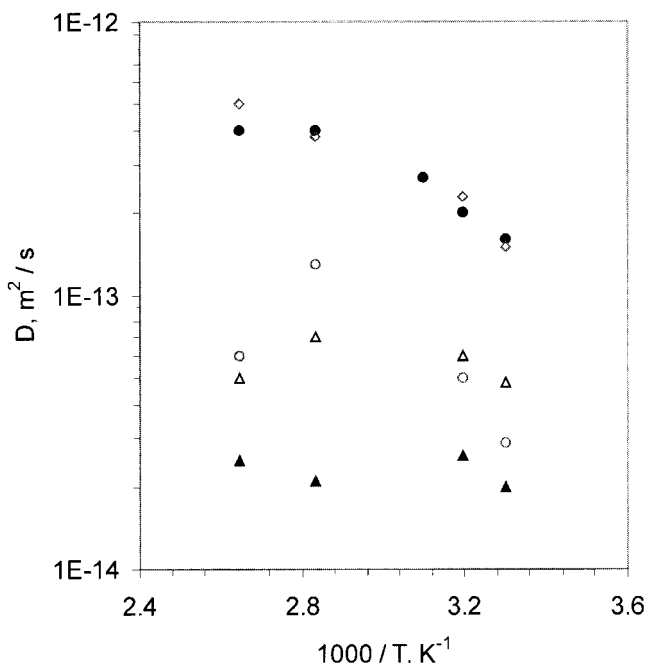


Figure 7 Effect of temperature on D for polyimides (water vapor pressure = 3168 Pa): (●) PMDA-50DDS/50ODA, (△) BPDA-50DDS/50ODA, (○) BPDA-DDS, (▲) BPDA-ODA, and (◇) DSDA-TPER.

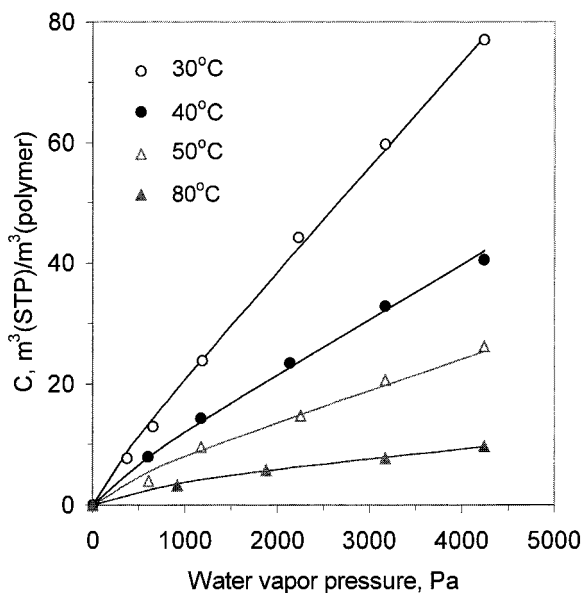


Figure 8 Effect of temperature on the sorption isotherms of PMDA-50DDA/50ODA.

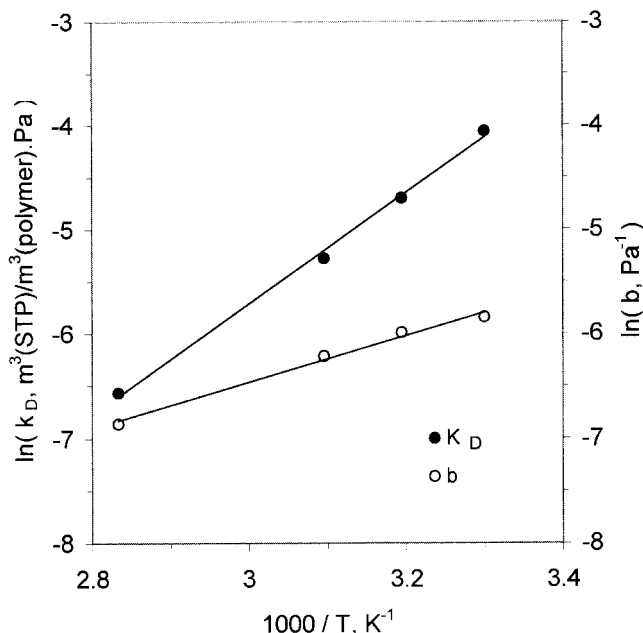


Figure 9 Van't Hoff plots of k_D and b for water vapor in the polyimide PMDA-50DDS/50ODA.

mentioned temperature dependence of the diffusion coefficient seems to be valid only from 30 to 80°C.

A detailed study of the isotherms was carried out for PMDA-50DDS/50ODA at different temperatures and different water vapor pressures. The experimental data were fit by dual-mode sorption curves, as shown in Figure 8. Table V gives the dual-mode sorption parameters at different temperatures. The parameters k_D and b are in good agreement with the van't Hoff analysis, as shown in Figure 9. The values of ΔH_D and ΔH_b , determined from the slopes of these semilogarithmic plots, are -44.31, and -18.46 kJ/mol, respectively.

Water vapor permeation

Table VI shows the water vapor permeability obtained from the sorption measurements at 30°C along with the average diffusion coefficient obtained from eq. (8) and the value of S obtained from the secant slope⁴¹ of the sorption isotherm for each membrane at a water vapor relative pressure of $p/p_s = 1$. PMDA-50DDS/50ODA shows greater water vapor permeation characteristics than other dense membranes. Water perme-

TABLE V
Dual-Mode Sorption Parameters of PMDA-50DDS/50ODA at Different Temperatures

Temperature (°C)	$k_D \times 10^3$ [m ³ (STP)/m ³ (polymer) Pa]	C'_H [m ³ (STP)/m ³ (polymer)]	$b \times 10^3$ (1/Pa)
30	17.26	4.93	3.0
40	9.07	3.87	2.5
50	5.10	4.05	2.1
80	1.40	4.41	1.0

TABLE VI
Parameters S , D , and P for Water Vapor in Dense Polyimide Membranes at 30°C and $p/p_s = 1$

Polyimide	$D \times 10^{14}$ (m ² /s)	S [mol/m ³ (polymer) Pa]	$P \times 10^{14}$ (mol m/m ² Pa s)
PMDA-50DDS/50ODA	16	0.81	12.96
BPDA-50DDS/50ODA	4.5	0.45	2.02
BPDA-DDS	3.8	0.64	2.43
BPDA-ODA	2.0	0.41	0.82
DSDA-TPER	16	0.29	4.64

ability in the membranes is in the following order at 30°C: BPDA-ODA < BPDA-50DDS/50ODA < BPDA-DDS < DSDA-TPER < PMDA-50DDS/50ODA. Table VII gives the water vapor permeabilities of these membranes measured at 85°C with a feed upstream pressure of 40 kPa and a permeate downstream pressure of 2 kPa. The permeability of water vapor in PMDA-50DDS/50ODA is almost 11 times higher than that of the BPDA-ODA membrane, and the permeability of water vapor in the dense polyimide membranes measured at 85°C is in the following order: BPDA-ODA < DSDA-TPER < BPDA-50DDS/50ODA < BPDA-DDS < PMDA-50DDS/50ODA. The orders of the permeability data given in Tables VI and VII agree with each other, with the one exception of DSDA-TPER. The permeability given in Table VII is, however, an order of magnitude higher because of the much higher temperature (85°C) and the much higher vapor pressure (40 kPa) at which the water permeation experiments were conducted.

CONCLUSIONS

Water vapor sorption and transport in five dense polyimide membranes have been studied by a gravimetric method. The sorption isotherms of water vapor in the polyimides have been successfully interpreted by both the dual-mode sorption model and the GAB model. Water vapor sorption and diffusion behaviors are nearly Fickian at higher water vapor activities, whereas non-Fickian diffusion has been observed at lower water vapor activities. This can be well described by the mechanism of combined Fickian and time-dependent diffusion. The diffusion coefficient and water vapor uptake in the polyimides are strongly dependent on the polymer molecular structure. At

TABLE VII
Permeability of Water Vapor in Dense Polyimide Membranes Measured at 85°C

Polyimide	$P \times 10^{13}$ (mol m/m ² Pa s)
PMDA-50DDS/50ODA	11.15
BPDA-50DDS/50ODA	4.36
BPDA-DDS	7.84
BPDA-ODA	1.04
DSDA-TPER	2.59

30°C and at a water vapor relative pressure of $p/p_s = 1$, the diffusion coefficient for the polyimides varies from 2.0×10^{-14} to 1.6×10^{-13} m²/s and is in the following order: BPDA-ODA < BPDA-DDS < BPDA-50DDS/50ODA < DSDA-TPER = PMDA-50DDS/50ODA. However, the water uptake varies from 1.57 to 4.37 wt % and is in the following order: DSDA-TPER < BPDA-ODA < BPDA-50DDS/50ODA < BPDA-DDS < PMDA-50DDS/50ODA. The order of the water vapor permeabilities predicted on the basis of sorption measurements at 30°C agrees very well with that obtained directly by permeation experiments at 85°C. Among the polyimide membranes studied in this work, DSDA-TPER is the only exception.

The technical help of Jin Yang (Université Laval) and the valuable advice of G. Chowdhury (Department of Chemical Engineering, University of Ottawa) are gratefully acknowledged.

NOMENCLATURE

α	first-order rate constant for the relaxation process (dimensionless)
a	water vapor activity (dimensionless)
A	GAB model parameter, temperature-dependent constant (dimensionless)
A_0	pre-exponential factor (dimensionless)
b	hole affinity constant (1/Pa)
B	GAB model parameter, temperature-dependent constant (dimensionless)
b_0	pre-exponential factor (1/Pa)
B_0	pre-exponential factor (dimensionless)
C	concentration or solubility of the penetrant in the polymer [m ³ (STP)/m ³ (polymer)]
C_D	concentration by normal dissolution [m ³ (STP)/m ³ (polymer)]
C_H	hole saturation constant [m ³ (STP)/m ³ (polymer)]
C_H'	maximum capacity of the polymer for the penetrant in the Langmuir sorption sites [m ³ (STP)/m ³ (polymer)]
C_m	monolayer moisture content [m ³ (STP)/m ³ (polymer)]
ΔH_b	enthalpy of sorption in the Langmuir environment (kJ/mol)

ΔH_D	enthalpy of sorption in the Henry's law environment (kJ/mol)
\underline{D}	diffusion coefficient (m^2/s)
\bar{D}	average diffusion coefficient (m^2/s)
D_E	equilibrium diffusion coefficient (m^2/s)
D_I	initial diffusion coefficient (m^2/s)
D_t	diffusion coefficient at time t (m^2/s)
H_L	heat of condensation of pure water (kJ/mol)
H_m	heat of monolayer sorption (kJ/mol)
H_n	heat of multilayer sorption (kJ/mol)
J	gas or vapor flux at the steady state ($\text{mol}/\text{m}^2 \text{ Pa s}$)
k	constant (dimensionless)
k_D	Henry's law solubility constant [$\text{m}^3(\text{STP})/\text{m}^3(\text{polymer}) \text{ Pa}$]
k_{D0}	pre-exponential factor [$\text{m}^3(\text{STP})/\text{m}^3(\text{polymer}) \text{ Pa}$]
L	thickness (m)
m	integer (dimensionless)
M_∞	equilibrium sorption [$\text{m}^3(\text{STP})/\text{m}^3(\text{polymer})$]
M_t	amount of vapor sorbed at time t [$\text{m}^3(\text{STP})/\text{m}^3(\text{polymer})$]
$M_{t,D}$	amount of vapor sorbed by Fickian diffusion [$\text{m}^3(\text{STP})/\text{m}^3(\text{polymer})$]
$M_{t,R}$	amount of vapor sorbed by non-Fickian diffusion because of relaxation [$\text{m}^3(\text{STP})/\text{m}^3(\text{polymer})$]
p	gas or vapor pressure (Pa)
P	permeability coefficient ($\text{mol m}/\text{m}^2 \text{ Pa s}$)
p_1	downstream or permeate side pressure (Pa)
p_2	upstream or feed side pressure (Pa)
p_s	vapor saturation pressure at a given temperature (Pa)
R	gas constant (J/mol K)
S	solubility coefficient [$\text{m}^3(\text{STP})/\text{m}^3(\text{polymer}) \text{ Pa}$]
t	time (s)
$t^{1/2}$	square root of time ($\text{s}^{1/2}$)
T	absolute temperature (K)
v	velocity of case II diffusion (m/s)
x	distance from the surface of the membrane (m)

References

- Overmann, D. C. U.S. Pat. 5,034,025 (1991).
- Rahimzadeh, R. A. U.S. Pat. 5,681,368 (1997).
- Cranford, R. J.; Roy, C.; Matsuura, T. *Can J Chem Eng* 1997, 75, 471.
- Chabot, S.; Roy, C.; Chowdhury, G.; Matsuura, T. *J Appl Polym Sci* 1997, 65, 1263.
- McCandless, F. P. *Ind Eng Chem Process Des Dev* 1972, 11, 470.
- Sacher, E.; Susko, J. R. *J Appl Polym Sci* 1979, 23, 2355.
- Coleman, M. R.; Kohn, R.; Koros, W. J. *J Appl Polym Sci* 1993, 50, 1059.
- Feng, X.; Sourirajan, S.; Tezel, H.; Matsuura, T. *J Appl Polym Sci* 1991, 43, 1071.
- Lokhandwala, K. A.; Nadakatti, S. M.; Stern, S. A. *J Polym Sci Part B: Polym Phys* 1995, 33, 965.
- Okamoto, K. I.; Tanihara, N.; Watanabe, H.; Tanaka, K.; Kita, H.; Nakamura, A.; Kusuki, Y.; Nakagawa, K. *J Polym Sci Part B: Polym Phys* 1992, 30, 1223.
- Okamoto, K.; Tanihara, N.; Watanabe, H.; Tanaka, K.; Kita, H.; Nakamura, A.; Kusuki, Y.; Nakagawa, K. *J Membr Sci* 1992, 68, 53.
- Lim, B. S.; Nowick, A. S.; Lee, K.; Viehbeck, A. *J Polym Sci Part B: Polym Phys* 1993, 31, 545.
- Seo, J.; Lee, A.; Lee, C.; Han, H. *J Appl Polym Sci* 2000, 76, 1315.
- Han, H.; Chung, H.; Gryte, C. C.; Shin, T. J.; Ree, M. *Polymer* 1999, 40, 2681.
- Han, H.; Seo, J.; Ree, M.; Pyo, S. M.; Gryte, C. C. *Polymer* 1998, 39, 2963.
- Vieth, W. R.; Sladek, K. J. *J Colloid Sci* 1965, 20, 1014.
- Patton, C. J.; Felder, R. M.; Koros, W. J. *J Appl Polym Sci* 1984, 29, 1095.
- Vieth, W. R. *Diffusion in and through Polymers: Principles and Applications*; Hanser: New York, 1991; Chapter 2.
- Anderson, R. B. *J Am Chem Soc* 1946, 68, 686.
- Bizot, H. In *Physical Properties of Foods*; Jowitt, R.; Escher, F.; Hallstrom, B.; Meffert, H. F. T.; Spiess, W. E. L.; Vos, G., Eds.; Applied Science: New York, 1983; p 43.
- Van den Berg, C. In *Properties of Water in Foods*; Simatos, D.; Multon, J. L., Eds.; Martinus Nijhoff: Dordrecht, 1985; p 119.
- Tsami, E.; Marinou-Kouris, D.; Maroulis, Z. B. *J Food Sci* 1990, 55, 1594.
- Lim, L.; Britt, I. J.; Tung, M. A. *J Appl Polym Sci* 1999, 77, 197.
- Jia, L.; Fu, H.; Xu, J.; Hirai, A.; Odani, H. *J Appl Polym Sci* 1994, 52, 29.
- Perrin, L.; Nguyen, Q. T.; Sacco, D.; Lochon, P. *Polym Int* 1997, 42, 9.
- Crank, J. *The Mathematics of Diffusion*, 2nd ed.; Oxford University Press: Oxford, 1975; Chapters 4 and 10.
- Berens, A. R.; Hopfenberg, H. B. *Polymer* 1978, 19, 489.
- Sun, Y.; Lee, H. *Polymer* 1996, 37, 3915.
- Sun, Y.; Lee, H. *Polymer* 1996, 37, 3921.
- Frisch, H. L. *Polym Eng Sci* 1980, 20, 2.
- Wang, T. T.; Kwei, T. K.; Frisch, H. L. *J Polym Sci Part A-2: Polym Phys* 1969, 7, 2019.
- Kwei, T. K.; Wang, T. T.; Zupko, H. M. *Macromolecules* 1972, 5, 645.
- Toi, K.; Ito, T.; Shirakawa, T.; Ikemoto, I. *J Polym Sci Part B: Polym Phys* 1992, 30, 549.
- Toi, K.; Ito, T.; Ikemoto, I.; Kasai, T. *J Polym Sci Part B: Polym Phys* 1992, 30, 497.
- Costello, M.; Koros, W. J. *J Polym Sci Part B: Polym Phys* 1995, 33, 135.
- Shigetomi, T.; Tsuzumi, H.; Toi, K.; Ito, T. *J Appl Polym Sci* 2000, 76, 67.
- Hao, J.; Tanaka, K.; Kita, H.; Okamoto, K. *J Polym Sci Part A: Polym Chem* 1998, 36, 485.
- Zimm, B. H. *J Chem Phys* 1953, 21, 934.
- Barrie, J. A.; Machin, D. *Trans Faraday Soc* 1971, 67, 244.
- Kesting, R. E.; Fritzsche, A. K. *Polymeric Gas Separation Membranes*; Wiley: New York, 1993; p 207.
- McHattie, J. S.; Koros, W. J.; Paul, D. R. *Polymer* 1991, 32, 840.